Interaction of Potential Vorticity Anomalies in Extratropical Cyclogenesis. Part II: Sensitivity to Initial Perturbations

ZONGHUI HUO

CMRP, School of Meteorology, University of Oklahoma, Norman, Oklahoma

DA-LIN ZHANG

Department of Meteorology, University of Maryland, College Park, Maryland

JOHN R. GYAKUM

Department of Atmospheric and Oceanic Sciences, McGill University, Montreal, Quebec, Canada

ABSTRACT

In Part I of this series of papers, the static potential vorticity (PV) inversion diagnostics are performed to examine the lateral and vertical interactions between two upper-level (northern and southern) troughs and their possible influences on the development of the March 1993 superstorm. This study continues the investigation of the relative importance of two PV anomalies associated with the short-wave troughs and their interaction in the surface cyclogenesis by considering their individual roles as an initial-value problem.

The piecewise PV inversion technique is first used to isolate the upper-level disturbances with a balanced vortex for each. The vortex is then either removed or its intensity doubled by subtracting the balanced vortex from or adding to the control initial conditions. With the modified initial conditions, a mesoscale model is integrated for 36 h to examine how each of the upper-level disturbances contributes to the surface development.

It is found that the northern and southern troughs play different roles in the surface cyclogenesis. Without the northern trough, the eastward propagation of the southern trough slows down and the surface development is severely impeded. More rapid cyclogenesis occurs when the northern trough's intensity is doubled. On the other hand, the deepening rate increases considerably when the southern trough is removed. Doubling the southern trough intensity slows the eastward progression of the northern trough and leads to a reduced deepening rate. In conclusion, the northern trough is crucial for the rapid development of the superstorm, whereas the southern trough is important only during the incipient stage of the cyclone. In particular, a much stronger surface cyclone could be spawned in the absence of the southern trough. This finding appears to contradict the previous work on the roles of trough mergers in extratropical cyclogenesis.

1. Introduction

The classical theory of baroclinic instability has been widely used in the past five decades to understand extratropical cyclogenesis during the cold season. The linear theory predicts an exponential growth of a single normal mode for a given baroclinically unstable mean state regardless of the type and structure of initial perturbations. However, many observations revealed the prevalence of traveling disturbances near the tropopause preceding the surface cyclogenesis and the presence of varying perturbation structures with respect to

Corresponding author address: Dr. Da-Lin Zhang, Department of Meteorology, University of Maryland, Room 3433, Computer and Space Science Building, College Park, MD 20742-2425.
E-mail: dalin@atmos.umd.edu

surface cyclones (Petterssen 1956; Sanders 1986, 1988; Uccellini 1990; Lefevre and Nielsen-Gammon 1995). Furthermore, the structures and intensity of these upper-level disturbances and their interactions with the low-level baroclinicity play important roles in determining the deepening rate and the final intensity of surface cyclones. Thus, relating these observations to baroclinic theory is not immediately obvious, particularly in estimating the deepening rate of surface cyclones. Studies by Farrel (1984, 1985, 1989) indicate that cyclogenesis should be considered as an initial-value problem, which was later demonstrated by the analysis of cyclone evolution in terms of upper- and lower-level disturbances (Rotunno and Fantini 1989; Whitaker and Barcilon 1992; Davis and Bishop 1994). This has led to a number of recent studies, ranging from modified baroclinic instability theories (Farrel 1994) to real-data case studies (Rotunno and Bao

1996), which attempt to reconcile the observations and theories.

It has been shown that the superstorm of 12–14 March 1993, hereafter referred to as the superstorm, deepened at a rate much larger than what baroclinic theory could predict (Huo et al. 1995; Kocin et al. 1995; Uccellini et al. 1995). The explosive development occurred as two upper-level short-wave troughs merged, resulting in a principal trough with back-shear tilt in the vertical (Huo et al. 1995; Bosart et al. 1996). Gaza and Bosart (1990) have noted from a composite analysis of 17 trough-merger cases that two-thirds of them tended to cause the explosively deepening of surface cyclones as defined by Sanders and Gyakum (1980). In addition, they found that the meridional tilt of the axis of the principal 500-hPa geopotential height trough changed from positive to negative prior to cyclogenesis, and that during the transition the two precursor 500-hPa vorticity maxima in the composite amalgamated into a single maximum and the 500-hPa trough amplitude nearly doubled.

Recently, Hakim et al. (1996) studied 1 of the 17 cases in Gaza and Bosart (1990) and observed that the trough merger is associated with a close approaching of the two upper-level precursor vorticity centers rather than an amalgamation. Using static piecewise inversion of quasigeostrophic potential vorticity, Hakim et al. (1996) investigated the lateral interaction between two upper-level PV anomalies (associated with a southern and a northern upper-level trough) and the background flow, and found that the background flow advection dominates the vortex–vortex interactions although the later becomes more robust as the two PV anomalies come closer. At 1000 hPa, the incipient cyclogenesis is forced by the background flow advecting the southern vortex. During the rapid surface cyclogenesis, advection of both vortices by the background flow contributes to geopotential height falls in the genetic area, and the nearest approach of the two troughs coincides with the timing of the most rapid deepening. With a simple model describing the two-vortex interaction in a background flow, Hakim et al. (1996) showed that the trough merger is extremely sensitive to small changes in the deformation field for a given set of initial conditions on the vortex position, size, and strength, suggesting limitations to the predictability of the merger phenomenon.

Using the static PV inversion, we have also shown in Part I of this series of papers (i.e., Huo et al. 1999) that the two short-wave troughs play an important role in determining the tropospheric flow structures associated with the superstorm. However, the impact of the vortex–vortex interaction and their interaction with the lower-level baroclinicity on the surface cyclogenesis is much more complicated than the static PV inversion can suggest since the disturbances interact with each other and the structures of initial perturbations vary with time. Thus, the objectives of the present study are to (i) investigate the individual effects of the two troughs on the cyclogenesis by treating the trough cyclogenesis as an initial-value problem, and (ii) evaluate the vortex–vortex interaction arguments discussed in Part I in a prognostic mode. Specifically, we will attempt to find an appropriate methodology to isolate the perturbations associated with each of the troughs and then remove one of them at a time from the model initial conditions. Subsequently, the Canadian regional finite-element (RFE) model will be integrated forward with the initial conditions so modified. Thus, the model integrations with the modified initial conditions will provide the sensitivity of the model cyclogenesis to the presence of only one of the perturbations. As part of the understanding, we will also examine the relative importance of dry versus moist dynamics in the development of the superstorm when only one of the troughs is present in the model initial conditions.

This paper is organized as follows. Section 2 describes the methodology to isolate the troughs from the model initial conditions. Section 3 presents the experiment design and section 4 shows various model initial conditions when one of the troughs is modified. Section 5 discusses results from the various sensitivity experiments and provides a prognostic evaluation of the vortex–vortex interaction. A summary and conclusions are given in the final section.

2. Isolating upper-level short-wave troughs

A few of the previous cyclogenesis studies have attempted to isolate the impact of various types of midtropospheric disturbances on the surface cyclogenesis. For example, Chen et al. (1983) employed a porous-sponge lateral boundary condition to prevent the eastward propagation of a large-scale trough into the model domain in a case of oceanic cyclogenesis. They concluded that the upper-level trough had relatively little impact since the lower-level development was only weakened but not prevented. Lapenta and Seaman (1992) tried to isolate the influence of the upper-level jet stream on surface cyclogenesis. In their procedure, they noted that special care must be taken to (a) prevent alteration of the initial low-level perturbations and (b) avoid disruption of the balance between the upper-level mass and wind fields. With this guidance, they conducted a series of sensitivity studies in which the model initial conditions are adjusted above 600 hPa to alternately weaken and strengthen the wind and mass fields associated with a polar jet by about 20% from the control simulation. While this approach considers the mass and wind balance, it still has limitations owing to the fact that the weakening (or strengthening) of the jet streak and its associated mass field is performed only for the levels above 600 hPa, and that the jet streak is closely related to the lower-level baroclinicity.

In the present study, we use the piecewise PV inversion technique of Davis and Emanuel (1991) to isolate the circulations associated with individual distur-

bances and then conduct sensitivity experiments to examine their relative importance in the development of the superstorm. The essence of this technique is based on the invertibility principle of PV, which allows one to obtain the balanced wind and mass fields associated with any PV perturbations. Thus, this technique can be utilized to effectively isolate the wind and mass fields associated with the two upper-level PV anomalies (or short-wave troughs) for the present study. Once the two troughs are isolated, they may be removed one at a time or both from the control model initial conditions. Since the inverted meteorological fields associated with the troughs are balanced, it will not introduce any ''significant noise'' into the initial conditions.

For the present study, we use the best model integration presented in Huo et al. (1998) that was initialized at 1200 UTC 12 March 1993 (hereafter referred to as 12/12–00) as the control simulation, which reproduces well the track and deepening rates of the superstorm as well as its associated prefrontal squall line and strong cold surge over the Gulf of Mexico. The balanced initial conditions are obtained by (i) calculating a mean PV field by averaging the 12-hourly Canadian Meteorological Centre's analysis of PV between 11/00 and 15/00, (ii) isolating the PV anomalies associated with the two short-wave troughs (see Fig. 1a) by subtracting the mean state, (iii) using the piecewise PV inversion to invert the PV anomalies and obtain their pertinent balanced wind and mass fields, and (iv) subtracting the balanced fields from (or adding to) the control initial conditions; see Part I for more details.

3. Experiment design

To properly examine the relative importance of the two troughs (hereafter referred to as the northern and southern troughs; see Fig. 1a) in the rapid development of the superstorm, 12 sensitivity experiments, including the control simulation (CTL), are carried out. All the simulations are initialized at 1200 UTC 12 March 1993 and integrated for 36 h. The results are then compared to the CTL simulation to examine the model sensitivity to varying initial conditions. Table 1 summarizes the experimental design.

The first two sensitivity experiments are designed to test the impact of removing either the northern or the southern trough from the control initial conditions on the surface cyclogenesis, while keeping all the other conditions and model parameters identical to the control simulation. They are referred to as NON (i.e., no northern trough) and NOS (i.e., no southern trough), respectively. Because of the record-breaking precipitation of the superstorm, three additional dry experiments, corresponding to the respective CTL, NON, and NOS, are performed, in which neither convective parameterization nor grid-scale precipitation is allowed. They are denoted as the control dry (CTLD), no northern trough dry (NOND), and no southern trough dry (NOSD), re-

spectively. The purpose of conducting the dry simulations is to separate the effects of diabatic heating from the large-scale baroclinic forcings on the cyclogenesis in the presence of only one or both troughs.

To evaluate whether or not the development of the superstorm is strongly related to the surface characteristics (i.e., land vs ocean), CTL and NOS are repeated except with modified surface characteristics (denoted as CTLG and NOSG); namely, the land surface to the east of 91°W and south of 45°N is replaced by an ocean surface. Again, two corresponding dry simulations (CTLGD and NOSGD) are performed to separate the relative importance of dry and moist dynamics in the surface development. Finally, in order to gain insight into the impact of varying intensity and locations of initial perturbations on the cyclogenesis, two additional simulations are performed in which the strength of the northern and southern trough in CTL is doubled; they are denoted as DON and DOS, respectively.

It should be mentioned that the above numerical experiments are designed only to isolate the influence of the two upper-level troughs on the surface cyclogenesis. These two troughs are not necessarily the most sensitive perturbations in determining the final intensity of the surface cyclone, according to recent adjoint modeling studies (e.g., Zou et al. 1998).

4. Varying model initial conditions

Figure 1 presents the model initial conditions for CTL, NON, NOS, DON, and DOS. The CTL initial conditions (Fig. 1a) show clearly the presence of two positively tilted short-wave troughs at 500 hPa: the northern trough (T_1) and the southern trough (T_2). In contrast, the northern (southern) trough is absent in the NON (NOS) initial conditions (cf. Figs. 1a–c), showing that the PV inversion scheme provides a reasonably clean removal of the height and wind fields associated with them from the CTL initial conditions. Note that the inverted height perturbation associated with the southern PV anomaly is only half of that associated with the northern PV anomaly (see dashed lines in Figs. 1b,c). Since the removal of a trough is equivalent to adding mass into an atmospheric column, the lower-level baroclinicity to the south of the anomaly is expected to decrease. In the present case, a comparison of Figs. 1a–c shows a more pronounced decrease of the lower-level baroclinicity (suggested by the 500-hPa height gradient) over the genesis area in the NON than the NOS initial conditions. This implies that there will be more available potential energy present in the NOS than the NON initial conditions, perhaps causing different final intensities of the storm. In the case of the DON (DOS) initial conditions, the northern (southern) trough is much stronger than that in the CTL because of doubling the height and wind perturbations associated with its pertinent PV anomaly (Figs. 1d,e).

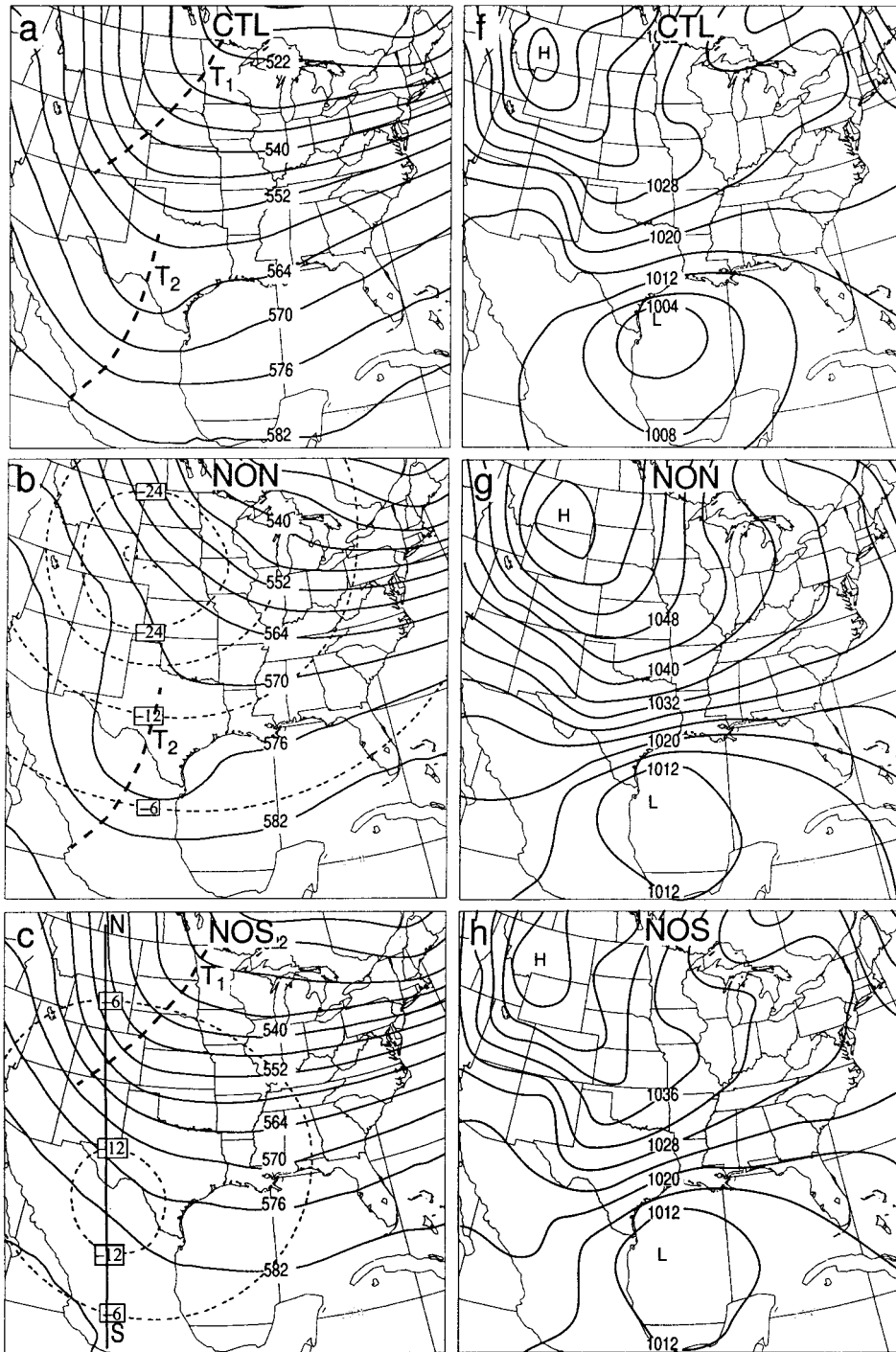Because of the changes of mass in a column, modi-

FIG. 1. (left panels) The 500-hPa geopotential height at intervals of 6 dam and (right panels) the sea level pressure at intervals of 4 hPa at the model initial time for experiments (a), (f) CTL, (b), (g) NON, (c), (h) NOS, (d), (i) DON, and (e), (j) DOS. Here, T_1 and T_2 show the positions of upper-level short-wave troughs.

fying the intensity of upper-level disturbances can alter substantially the structure and strength of the surface pressure perturbations. For example, the initial intensity of the surface cyclones in both the NON and NOS is decreased by 10 hPa and their centers are shifted about 300 km southward (cf. Figs. 1f–h). These changes in intensity and position occur because of the replaced cold air mass to the north that hydrostatically leads to the production of higher pressures at the lower levels and spreads to a wide area by the Laplacian operator in the
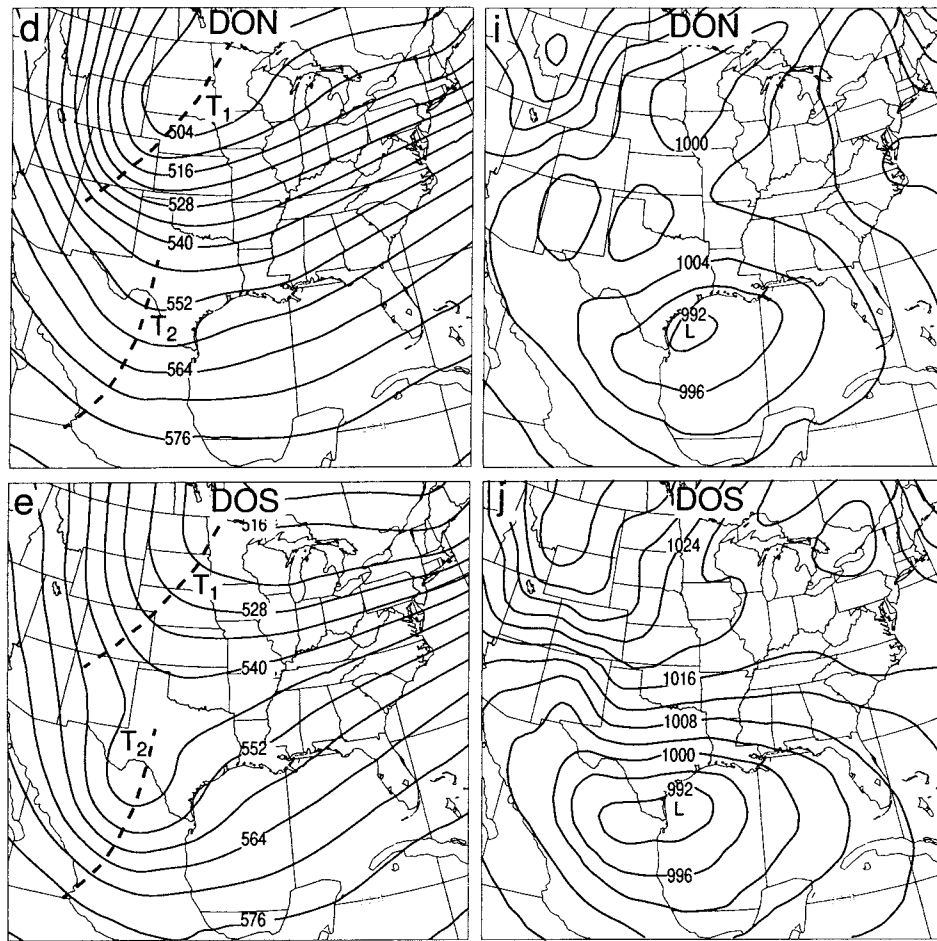
FIG. 1. (*Continued*) Line NS shows the location of the vertical cross section used in Fig. 2. Dashed lines in (b) and (c) denote the distribution of the inverted height perturbation (at 500 hPa) associated with troughs T_1 and T_2, respectively.

PV inversion. On the contrary, the doubling of the trough intensity is equivalent to evacuating mass from the column, resulting in the increased low-level baroclinicity in the genesis area (Figs. 1d,e) and over 12 hPa deeper central pressure of the cyclone under study

TABLE 1. Experiment design.

Experiment	Remarks
CTL	Control simulation
NON	Northern trough is removed
NOS	Southern trough is removed
CTLD	Same as CTL but no latent heating is allowed
NOND	Same as NON but no latent heating is allowed
NOSD	Same as NOS but no latent heating is allowed
CTLG	Same as CTL but surface characteristics are modified
NOSG	Same as NOS but surface characteristics are modified
CTLGD	Same as CTLG but no latent heating is allowed
NOSGD	Same as NOSG but no latent heating is allowed
DON	Northern trough intensity is doubled
DOS	Southern trough intensity is doubled

(Figs. 1i,j). Because of the substantial removal of air mass in DON, the initial sea level pressure field shows a zone of southwest–northeast-oriented trough parallel to the northern trough axis at 500 hPa (cf. Figs. 1d,i). The modification of this set of initial conditions appears to be most pronounced among all the sensitivity experiments. Nevertheless, the basic surface pressure pattern and the cyclone center are well preserved in both the DON and DOS initial conditions (Figs. 1i,j).

To quantify further the magnitude of the removed mass and wind fields, Fig. 2 shows north–south vertical cross sections of geopotential height, temperature, and section-normal winds that are inverted from the PV anomaly associated with the southern trough; they are exactly the differences between the CTL and NOS initial conditions (i.e., CTL minus NOS). It is evident that more pronounced differences occur at the upper levels, that is, with the maximum height perturbation of 230 m near 300 hPa, the maximum cooling of 6.5°C at 500 hPa, and the maximum cyclonic winds of 20 m s^{-1} at 300 hPa. Note that the maximum height perturbation at
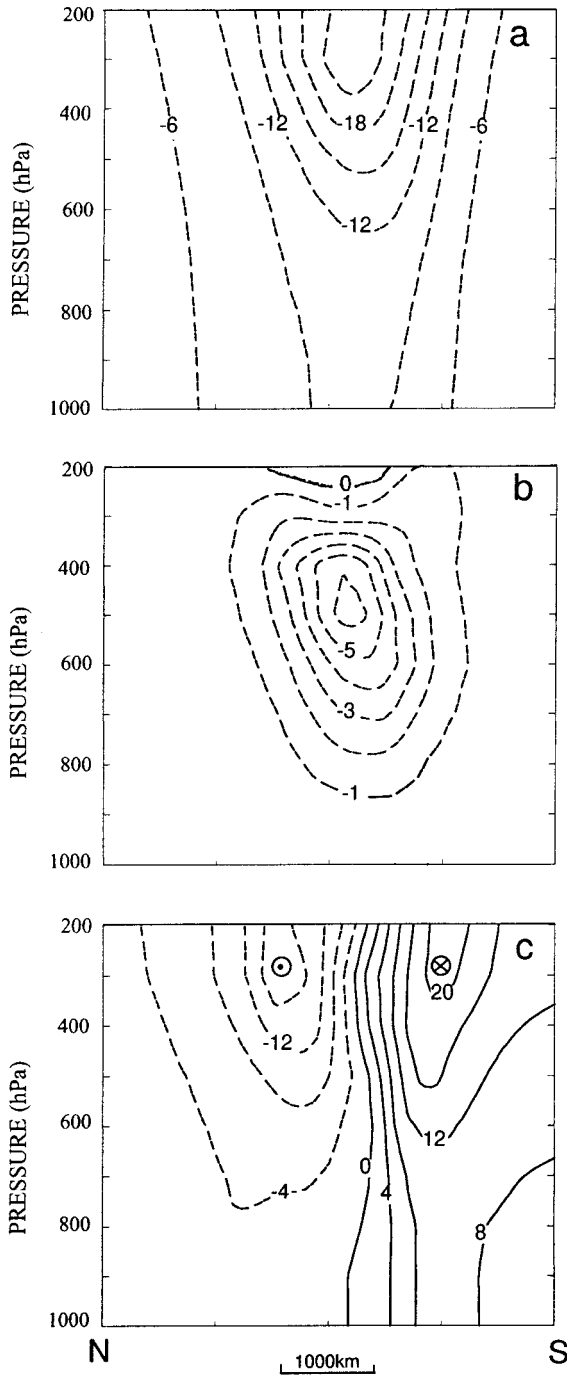
FIG. 2. North–south vertical cross sections of (a) geopotential height (dam), (b) temperature (°C), and (c) section-normal winds [m s^{-1}, positive (negative) values denote flows into (out of) the page] that are inverted from the southern PV anomaly. It is taken along line NS in Fig. 1c.

300 hPa is hydrostatically associated with weak warming above (<1.0°C) and strong cooling below. Note also that the influence of the upper-level perturbations decreases rapidly downward with little changes in tem-
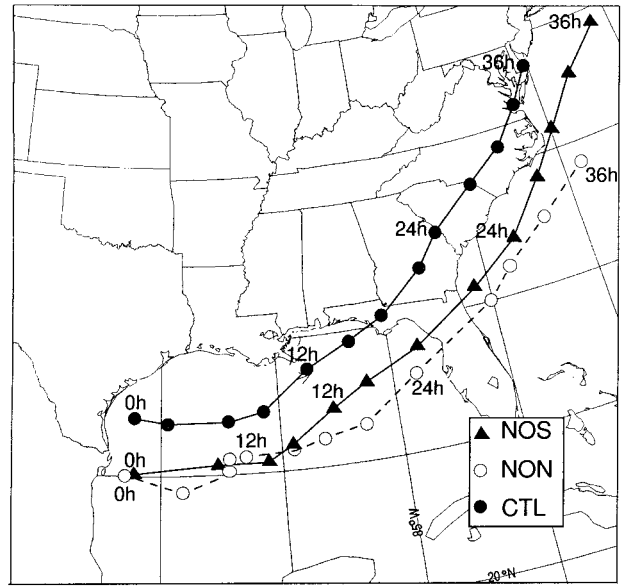
FIG. 3. The predicted tracks from expts CTL (solid circles), NON (triangles), and NOS (open circles).

perature and winds below 800 hPa. Thus, the initial conditions so obtained are dynamically meaningful since we are only interested in the sensitivity of the surface cyclogenesis to the upper-level perturbations. Similar vertical structures exist for the northern trough (not shown), but with the magnitude much greater than that of the southern trough.

5. Results

In this section, the RFE model is integrated for 36 h using the various initial conditions discussed in the preceding section. The sensitivity of the model integrations will be evaluated in terms of the evolution of the upper-level disturbances, the tracks and central pressures of the surface cyclones, as well as their quantitative precipitation. The central mean sea level pressure is used here as an indication of the storm's intensity although it does not always provide the most accurate measure of the storm's development. For the sake of subsequent discussions, Figs. 3 and 4 show, respectively, the track and the central pressure traces of the surface cyclone from CTL and other sensitivity simulations. The superstorm was initiated over the coast of Texas and then it deepened 26 hPa as it traveled northeastward during the 36-h integration period. The storm was in the mature stage at 14/00–36 and it still continued to deepen subsequently in both the observations and the model prediction (see Huo et al. 1995). The effects of latent heat release versus large-scale baroclinicity on the cyclogenesis are assessed by comparing the deepening of the cyclone between CTL and CTLD. In the absence of diabatic heating, the modeled minimum central pressure is 985 hPa compared to 974 hPa in CTL at the end of
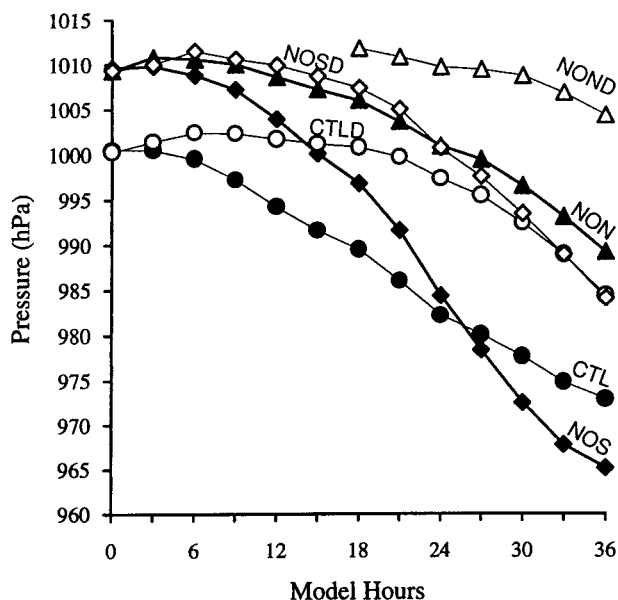
FIG. 4. Time traces of central sea level pressure for all the sensitivity experiments except for expts DOS and DON.

the 36-h integration. This indicates that diabatic heating accounts for about 42% of the total deepening, which is similar to that (40%) obtained with the integration initialized at 0000 UTC 13 March (Huo et al. 1995).

a. Prognostic evaluation of the vortex–vortex interaction

Removal of the two troughs one at a time will allow us to evaluate indirectly the vortex–vortex interaction arguments obtained from the static PV inversion in Part I. It is still possible that the perturbation would reappear if, after the removal, there is an instability. Furthermore, it is necessary to make sure that the removed perturbations will not recover as a distinct entity during the course of integration before we can analyze the evolution of the remaining disturbances in relation to the surface development. For these purposes, Fig. 5 shows the 12- and 24-h predictions of 400-hPa PV for NON, NOS, DON, and DOS. In the case of removing the northern trough (NON), the model still produces a PV perturbation to the north but, on average, with 1 PVU weaker than that in CTL (see Figs. 5a,b). The generation of this PV anomaly is attributable partly to the imperfect isolation of the anomaly associated with the northern trough using the 30% relative humidity criterion and partly to the continued descent and southward advection of stratospheric air. Nevertheless, in the absence of the strong northern perturbation, the southern PV anomaly moves much slower than that in the CTL, which is consistent with the analysis of the vortex–vortex lateral interaction presented in Part I. Note the different positions of the remaining PV anomaly with respect to the cyclone center between NON and CTL, which shows clearly the

reduced influence of the upper-level perturbations on the surface cyclogenesis in NON.

The removal of the southern trough (NOS) is relatively straightforward as compared to that in NON, and there is little evidence of a reappearance of the southern PV anomaly during the 36-h integration (Figs. 5c,d). As discussed in Part I, the flow associated with the southern PV anomaly tends to slow the southeastward propagation of the northern trough. This is confirmed with NOS, which shows relatively faster eastward movement of the northern trough, as compared to that in CTL.

When the northern trough is doubled in intensity (DON), the southern trough moves faster than that of the CTL (Figs. 5e,f) since the eastward advection of the southern trough is enhanced as compared to the CTL. In contrast, in the case of doubling the southern trough (DOS), the northern trough moves slower than that of CTL (cf. Figs. 5g,h) because the stronger westward winds associated with the doubled southern PV anomaly cancel part of the large-scale eastward advection of the northern trough. All these results are consistent with the vortex–vortex interaction conclusion based on the static PV inversion as discussed in Part I. As will be seen in the next subsection, the differences in the propagation of the upper-level troughs determine the movement and the intensification of the surface cyclone.

b. Sensitivity to the northern trough

As shown in Figs. 1b and 1g, removing the northern trough shifts the center of the NON cyclone about 300 km southward due to the rearrangement of the mass field. Correspondingly, the 36-h integration produces a cyclone track that is about 300 km to the right of the CTL one, which places the cyclone center offshore rather than over the land along the coast during the development period (Fig. 3). This implies that the NON cyclone tends to access warmer and moister air from tropical regions, producing more precipitation if its intensity were the same as that in CTL. However, because of the slower eastward progression of the upper-level short-wave (T_2) forcing in the absence of the vortex–vortex interaction, the surface cyclone is about 16 hPa weaker and 250 km slower than the CTL one at the end of the 36-h integration (Figs. 3 and 4); 68% of the weakening (i.e., 11 hPa) is associated with the removal of the northern trough at the model initial time (cf. Figs. 1g and 4). Moreover, the negative tilt of upper-level height perturbation, seen in CTL and most of the trough-merger cases (Gaza and Bosart 1990), does not appear. Of interest is that despite the weak development, its associated quantitative precipitation is close to that in CTL. In addition, the observed prefrontal squall line is reasonably reproduced [cf. Fig. 10c in Huo et al. (1998) and Fig. 6 herein] only with a slight phase lag. These similarities indicate that the northern trough does not have an important influence on the development of the
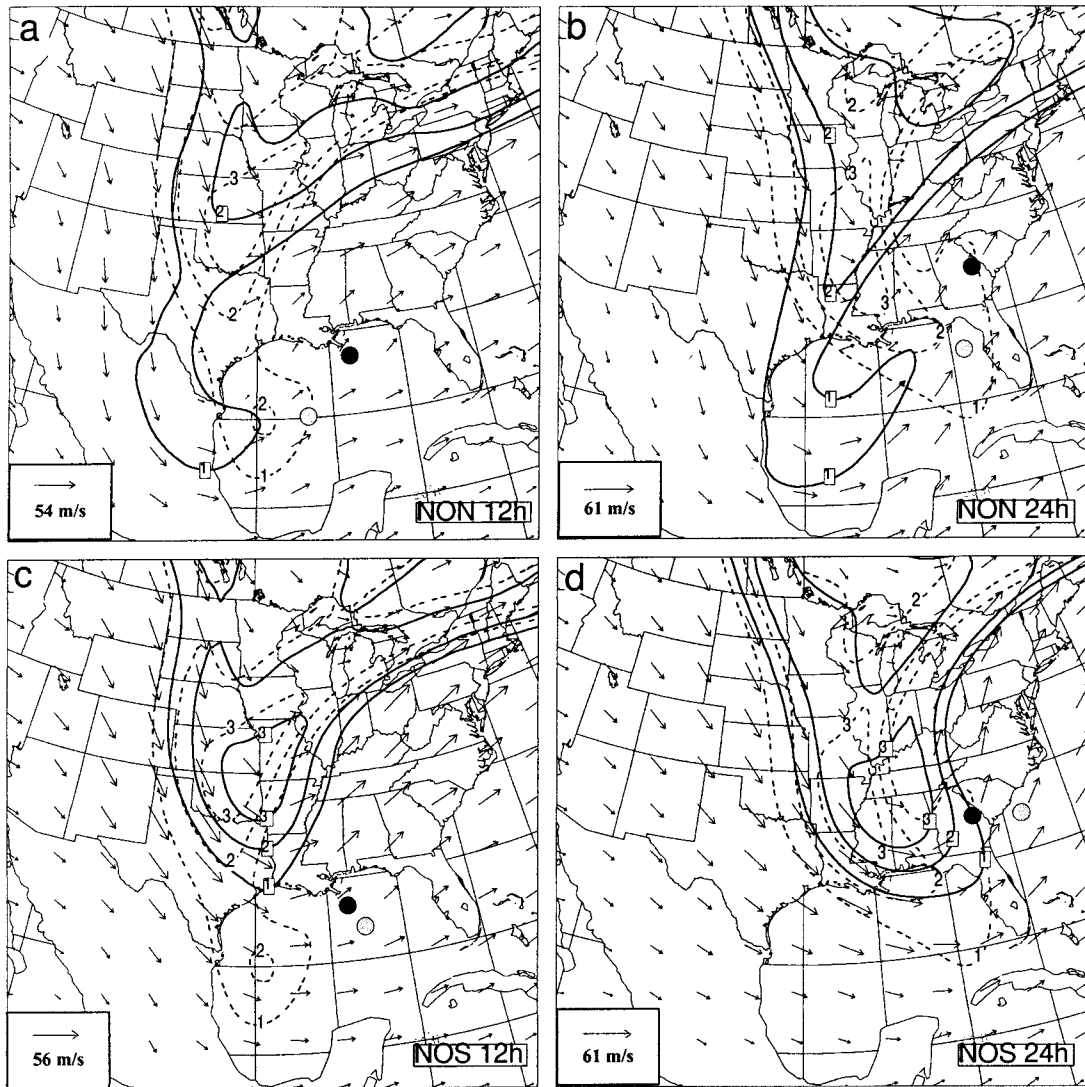
FIG. 5. Left (right) panels show the 12-h (24-h) predictions of 400-hPa PV (solid) at intervals of 1 PVU, superposed with wind vectors (its maximum value is given in inset) for (a), (b) NON, (c), (d) NOS, (e), (f) DON, and (g), (h) DOS runs. Dashed lines denote the 400-hPa PV for the control simulation. Solid and shaded circles give the cyclone centers for CTL and each sensitivity experiment, respectively.

prefrontal squall line and its associated precipitation, since its removal affects little the thermal structure and static stability in the warm sector as well as the frontal forcing. It follows that the weaker NON cyclone is mainly due to the reduced baroclinic (dry dynamical) contribution. In other words, the southern trough alone cannot generate this superstorm.

When diabatic heating is not allowed (NOND), the model fails to produce a tight, closed circulation until 18 h into the integration despite a closed cyclone in the model initial condition (cf. Figs. 1g and 4). An examination of 3-hourly model outputs shows a continued filling of the cyclone during the first 3–6-h integration. The filling scenario occurs in all the dry simulations, including the CTLD (Fig. 4). This appears

to be attributable to the "sudden removal" of latent heat release. Specifically, the initial conditions were derived from the observational analysis that contains the effect of latent heat release. When the latent heat release is turned off "suddenly," all dynamics fields will adjust according to the dry regime, leading to weakening vertical motion and low-level convergence. It is apparent from Fig. 4 that the cyclone deepens only 5 hPa at the end of the 36-h integration, which is the weakest one among all the sensitivity experiments. A comparison of the deepening rates between NOND and CTLD reveals again the important baroclinic contribution of the northern trough to the CTL surface cyclogenesis. Thus, the latent heat release in the absence of the northern trough, particularly in the vicinity of
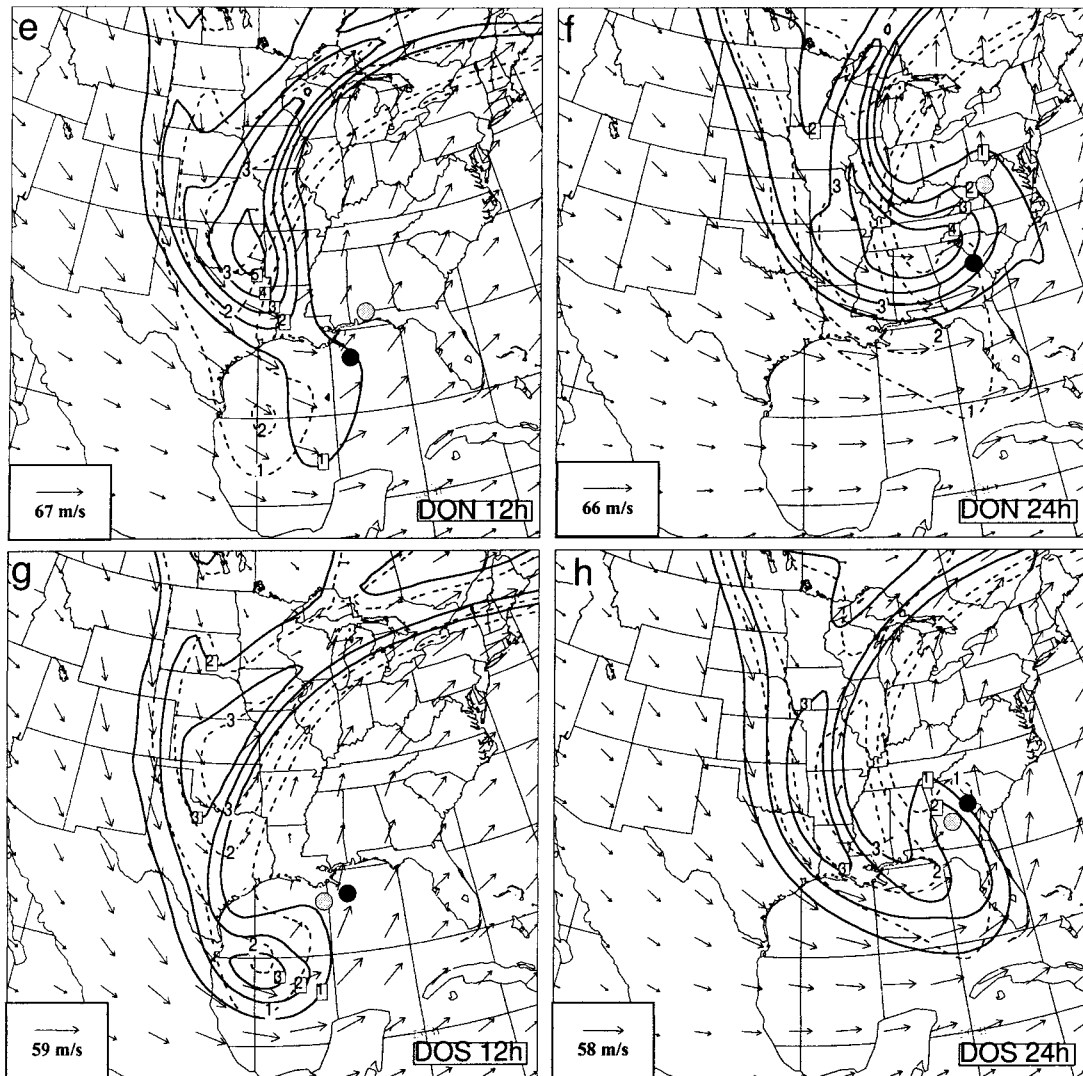
FIG. 5. (*Continued*)

the cyclone center (Fig. 6), plays an important role in the organization and deepening of the superstorm during its incipient stage.

c. Sensitivity to the southern trough

The rearrangement of the mass field after the removal of the southern trough (NOS) produces an initial location, intensity, and a subsequent cyclone track similar to those in NON, that is, about 10 hPa weaker and 300 km southward shift from the CTL one (Figs. 3 and 4). But surprisingly, the NOS deepens at a rate much faster than any of the sensitivity tests, including the CTL (Fig. 4). Although the NOS cyclone begins with a 10-hPa weaker central pressure, it becomes 8 hPa deeper than the CTL one by the end of the 36-h integration. This result, which may be case dependent, appears to contradict with the important roles of trough mergers in the rapid surface cyclogenesis as hypothesized by Gaza and Bosart (1990).

A natural question is: How could such a strong cyclone develop in the absence of the southern trough? Three such factors come to mind before we can address the above question: (i) the diabatic heating due to the access of more tropical high-θ_e air, (ii) the surface characteristics due to its track offshore, and (iii) the upper-level adiabatic forcings due to the absence of the southern trough. First, a comparison between NOS and NOSD show a pronounced (44%) contribution due to the latent heat release to the cyclogenesis; it produces a 19-hPa difference in central pressure. The 24-h accumulated precipitation also displays heavier precipitation along the path of the NOS cyclone than that in the CTL one (Fig. 7). This increased precipitation is more likely a
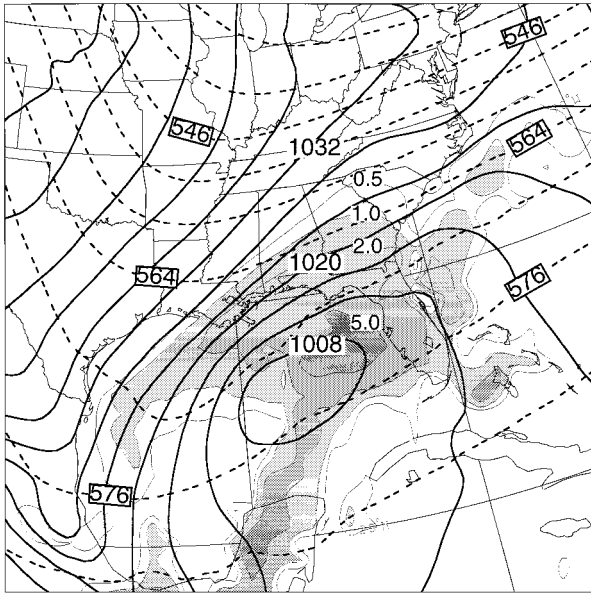
FIG. 6. The 18-h NON forecast of 500-hPa height (dashed lines) at intervals of 6 dam, sea level pressure (solid lines) at intervals of 4 hPa and precipitation rate (mm h^{-1}).

consequence of the positive feedback among the dynamical forcing, moisture convergence, latent heat release, and rapid deepening of the storm.

The impact of the surface characteristics on the cyclogenesis is examined by rerunning CTL and NOS but with the eastern half of the United States being treated as ocean (i.e., CTLG and NOSG). A comparison of these two runs reveals that the underlying surface characteristics only make a small positive contribution (2–3 hPa) to the deepening of the superstorm (not shown). Thus, we may ignore the impact of the surface characteristics on the surface development.

While the diabatic heating plays an important role in producing the more rapid deepening of the surface cyclone, it does not seem to be the driving parameter in determining the rapid development, since the NON cyclone, having an initial intensity and a track similar to the NOS cyclone's, does not exhibit such a deepening tendency. In particular, the more rapid deepening tendency also occurs in the absence of the diabatic heating, as can be seen by comparing the two dry runs between CTLD and NOSD. Although the final intensity in the two dry runs happens to be nearly the same, the NOSD cyclone deepens at a rate much faster than that in CTLD owing to their different initial intensities (Fig. 4). This suggests that the more rapid deepening tendency should be discussed in the context of dry dynamics. Specifically, *the absence of the southern trough allows the northern one to propagate faster toward the surface cyclone center, as mentioned previously, thereby facilitating the vertical coupling of cyclonic vorticity and the spinup of the surface cyclone.*

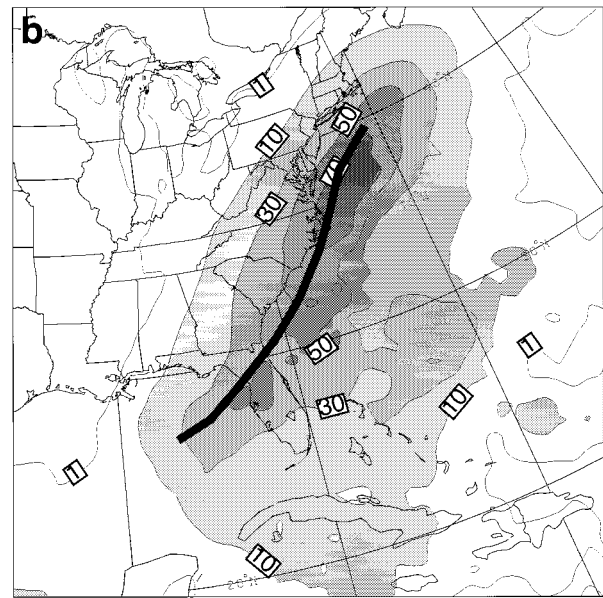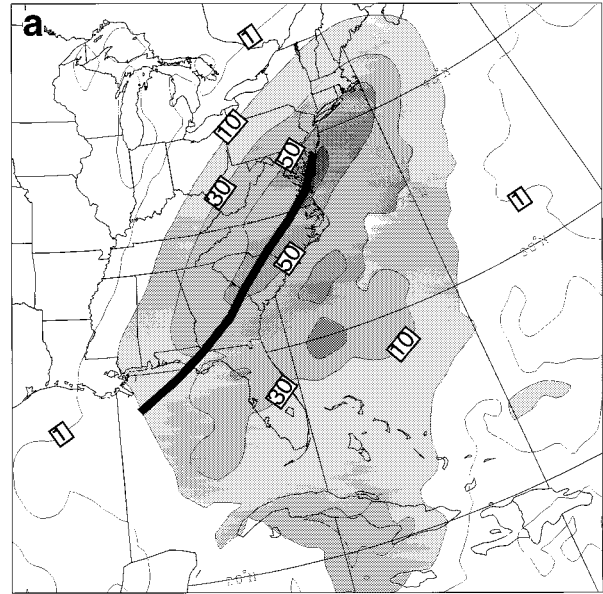To substantiate the above point, we apply the static

FIG. 7. The 24-h precipitation accumulation (mm) ending at 36 h for (a) CTL and (b) NOS runs.

piecewise PV inversion technique to the 6-hourly model outputs of the CTL and NOS integrations. First, the total PV perturbations are partitioned into the following four components: (i) the stratosphere-related PV perturbations (Q_d), (ii) the lower-tropospheric PV perturbations associated with condensational heating (Q_h), (iii) the effective lower boundary (θ_{eff}), and (iv) the remaining interior PV perturbations that are not included in the above three components (Q_r). See Part I for a detailed description of the PV partitioning. Contributions of each component to the 1000-hPa geopotential height at the cyclone center are then calculated. As shown in Table 2, all contributions in the two runs increase with time,

TABLE 2. The absolute (dam) and relative (%) contributions of various PV anomalies to the 1000-hPa height at the center of the surface cyclone from expts CTL and NOS.

Day/h	Q_d dam (%)		Q_h dam (%)		θ_{eff} dam (%)		Q_r		Total	
	CTL	NOS	CTL	NOS	CTL	NOS	CTL	NOS	CTL	NOS
12/12	−11.0 (40.1)	−3.8 (20)	−6.0 (21.9)	−5.2 (26)	−10.4 (37.9)	−11.0 (55)	10.9	11.4	−17.1	−8.6
12/18	−12.2 (37.2)	−5.3 (24)	−6.3 (19.2)	−4.5 (20)	−14.3 (43.6)	−12.4 (56)	15.2	12.9	−17.8	−9.2
13/00	−19.1 (39.7)	−11.7 (35)	−10.3 (21.4)	−7.0 (21)	−18.7 (38.9)	−14.9 (44)	25.1	18.9	−23.0	−14.7
13/06	−27.8 (47.0)	−20.2 (46)	−13.4 (22.6)	−10.0 (23)	−18.0 (30.4)	−13.5 (31)	31.5	22.6	−27.7	−21.1
13/12	−39.0 (52.1)	−32.2 (51)	−16.4 (21.9)	−15.1 (24)	−19.4 (25.9)	−16.3 (26)	41.7	31.9	−33.1	−31.7
13/18	−47.3 (52.5)	−44 (49)	−16.7 (18.5)	−21.2 (24)	−26.1 (29.0)	−25.2 (28)	52.7	45.6	−37.4	−44.8
14/00	−53.4 (53.0)	−52.2 (49)	−19.2 (19.1)	−21.7 (21)	−28.1 (27.9)	−31.8 (30)	60.3	56.2	−40.8	−49.5

which is consistent with the rapid development of the cyclones. Because of the removed southern trough, the magnitude of the upper-level dry PV and its contribution to the surface cyclone are reduced by over 60% in the first 12-h integration. Moreover, due to the southeastward acceleration of the northern trough in the absence of the southern one, the Q_d contribution in NOS catches up quickly with that in CTL, reaching −522 m as compared to −534 m by the end of the 36-h integration. Similarly, both the Q_h and θ_{eff} contributions in NOS, starting with smaller magnitudes, grow more rapidly with time than those in CTL. As a result, the net contribution of all the PV anomalies to the cyclogenesis in NOS increases from −86 m to −495 m (a net increase of −409 m), whereas in CTL it only increases from −171 m to −408 m (a net increase of −237 m). The net increase for the NOS cyclone nearly doubles the CTL one. In terms of the relative importance, the upper-level forcing (Q_d) in NOS (from −38 to −522 m) plays a more important role in the surface cyclogenesis than that in CTL (from −110 to −534 m).

To help relate the above PV-inverted contributions to the deepening of the storm shown in Fig. 4, the 6-h rate of these contributions given in Table 2 is presented in Fig. 8, which shows essentially the contributions of the various PV anomalies to the cyclone's average deepening rates from NOS and CTL. It is evident that the net contribution to the rate of height fall of the NOS storm is consistent with the deepening rate inferred from Fig. 4. An examination of the individual contributions in NOS reveals that the upper-level perturbations (Q_d) contribute the most, followed by the lower-level thermal advection (θ_{eff}) and diabatic heating (Q_h). The rate of changes also shows more significant differences in all the PV contributions after the 15-h integration between CTL and NOS.

d. Sensitivity to the doubling of the northern and southern troughs

When either the northern (DON) or the southern (DOS) trough is doubled in intensity, it affects little the cyclone tracks except that the DON (DOS) cyclone moves relatively faster (slower) than the CTL one (not shown). Although the initial central pressures of the DON and DOS cyclones are reduced by nearly the same amount (i.e., 10 hPa; see Figs. 1i,j), they experience quite different deepening. Specifically, the DON cyclone deepens at a rate faster than that of CTL and its solution tends to converge toward the CTL one, whereas the DOS cyclone spins up very slowly; its rate is even slower than that in CTL (see Figs. 9 and 10). It is easy to understand why doubling the northern trough would give rise to a stronger surface cyclone. But one would wonder why the same scenario does not occur with the DOS cyclone if the trough-merger mechanism proposed by Gaza and Bosart (1990) is operative. This issue can be addressed in the context of the upper-level vortex–vortex lateral interactions as well as their vertical interactions. That is, doubling the southern trough tends to slow further the eastward progression of the northern trough (see Figs. 5g,h), thereby leading to the decreased coupling with and the reduced deepening of the cyclone compared to that in CTL. Therefore, doubling the southern trough only produces a deeper cyclone at the initial time, but it does not favor the subsequent deepening of the cyclone.

In contrast, doubling the northern trough tends to advect the PV anomaly associated with the southern trough faster toward the surface cyclone, and increase its influence on the cyclogenesis through advection by the large-scale background flow. Thus, both processes favor the generation of a stronger cyclone. The results confirm the conclusions obtained in Part I and the foregoing subsections that *the northern trough is more crucial to*
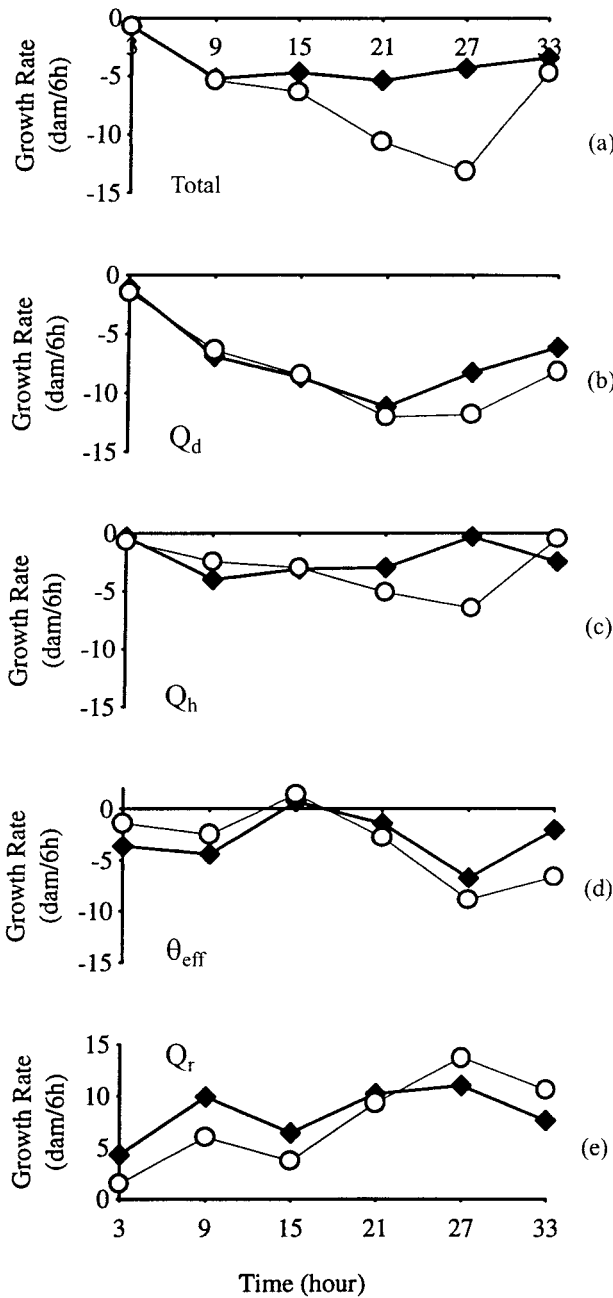
FIG. 8. The contributions to 1000-hPa height change (dam/6 h) from (a) the total PV anomaly, (b) the upper-level dry PV anomaly Q_d, (c) the lower-level moist PV anomaly Q_h, (d) the effective bottom boundary anomaly θ_{eff}, and (e) the remaining PV anomaly Q_r for CTL (thick lines) and NOS (thin lines).

the present cyclone development, and the southern trough only plays a role in organizing the cyclonic circulations during the incipient stage.

6. Summary and conclusions

In this study, the relative importance of two upper-level troughs in the development of the superstorm of
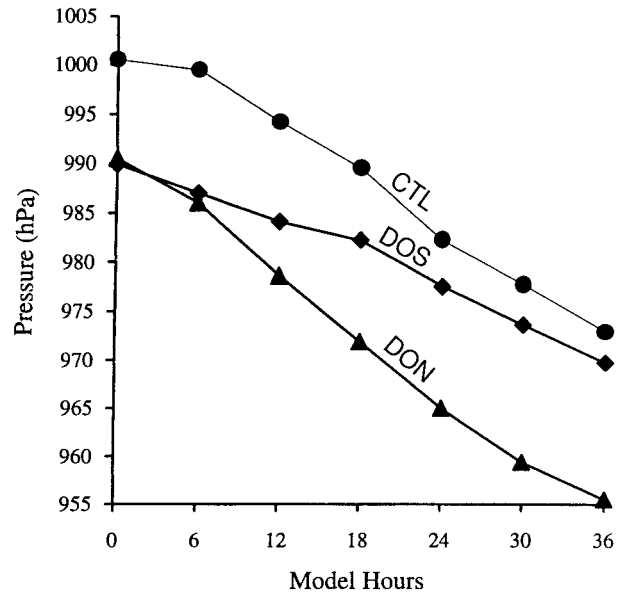

FIG. 9. As in Fig. 4 but for CTL, DON, and DOS runs.

March 1993 is further investigated, following the static PV analysis given in Part I, by considering their individual impacts as an initial-value problem. To provide a clean isolation of various PV anomalies, the piecewise PV inversion is used to produce the balanced wind and mass fields associated with the troughs. This approach appears to be more realistic than any other techniques in the literature for performing this type of sensitivity experiments. By removing or changing the intensity of the troughs in the model initial conditions, the RFE model is integrated to examine the impact of each trough on the storm development.

It is found that the advections of the northern and southern troughs toward the cyclone are important to the surface cyclogenesis. Without the northern trough, the advection of the southern trough toward the cyclone decreases and the surface development is severely impeded. With the doubling of the northern trough, the advections of both the southern trough by the northern PV anomaly and the northern trough by the background
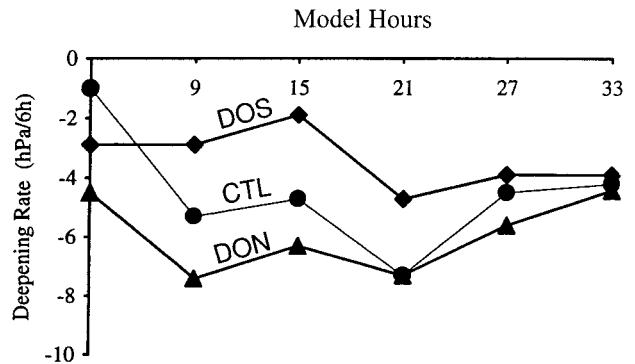

FIG. 10. As in Fig. 8a but for CTL, DON, and DOS runs.

flow increase and the surface cyclogenesis is enhanced. However, the doubling of the southern trough slows the eastward progression of the northern trough, giving rise a reduced deepening rate of the cyclone. Of interest is that *a stronger cyclone develops in the case of removing the southern trough.* Most of the above results confirm the findings based on the static PV inversion in Part I. Of further interest is that *despite the pronounced model sensitivity to the intensity of the superstorm, the large changes in perturbations do not affect significantly the track of the storm,* indicating the importance of the background flow in determining the storm's track. In conclusion, we may state that *in the present case the northern trough is instrumental in the rapid development of the superstorm, because it is stronger, and more importantly, it tends to be better coupled with the surface disturbance than the southern counterpart, especially when the southern trough were absent. The southern trough plays an important role only in the initial organization of the cyclone.* The results indicate that in some trough-merger cases the short-wave vortex–vortex interaction does not necessarily lead to the development of a more intense surface cyclone. Of course, more case studies of trough mergers along this line have to be performed before the above conclusions can be generalized.

REFERENCES

Bosart, L. F., G. J. Hakim, K. R. Tyle, M. A. Bedrick, W. E. Bracken, M. J. Dickinson, and D. M. Schultz, 1996: Large-scale antecedent conditions associated with the 12–14 March 1993 cyclone (''Superstorm '93'') over eastern North America. *Mon. Wea. Rev.,* **124,** 1865–1891.

Chen, T. C., C. B. Chang, and D. J. Perkey, 1983: Numerical study of an AMTEX '75 oceanic cyclone. *Mon. Wea. Rev.,* **111,** 1818–1829.

Davis, C. A., and K. A. Emanuel, 1991: Potential vorticity diagnostics of cyclogenesis. *Mon. Wea. Rev.,* **119,** 1929–1953.

Davis, H. C., and C. H. Bishop, 1994: Eady edge waves and rapid development. *J. Atmos. Sci.,* **51,** 1930–1946.

Farrell, B., 1984: Modal and nonmodal baroclinic waves. *J. Atmos. Sci.,* **41,** 668–673.

——, 1985: Transient growth of damped baroclinic waves. *J. Atmos. Sci.,* **42,** 2718–2727.

——, 1989: Optimal excitation of baroclinic waves. *J. Atmos. Sci.,* **46,** 1193–1206.

——, 1994: Evolution and revolution in cyclogenesis theory. *The Life Cycles of Extratropical Cyclones,* Vol. I, Aase Grafiske A/S, 101–110.

Gaza, R. S., and L. F. Bosart, 1990: Trough-merger characteristics over North America. *Wea. Forecasting,* **5,** 314–331.

Hakim, G. J., D. Keyser, and L. F. Bosart, 1996: The Ohio Valley wave-merger cyclogenesis event of 25–26 January 1978. Part II: Diagnosis using quasigeostrophic potential vorticity inversion. *Mon. Wea. Rev.,* **124,** 2176–2205.

Hoskins, B. J., M. E. Mcintyre, and R. W. Robertson, 1985: On the use and significance of isentropic potential vorticity amps. *Quart. J. Roy. Meteor. Soc.,* **111,** 877–946.

Huo, Z., D.-L. Zhang, J. R. Gyakum, and A. N. Staniforth, 1995: A diagnostic analysis of the superstorm of March 1993. *Mon. Wea. Rev.,* **123,** 1740–1761.

——, ——, and ——, 1998: An application of potential vorticity inversion to improving the numerical prediction of the March 1993 superstorm. *Mon. Wea. Rev.,* **126,** 424–436.

——, ——, and ——, 1999: Interaction of potential vorticity anomalies in extratropical cyclogenesis. Part I: Static piecewise inversion. *Mon. Wea. Rev.,* **127,** 2546–2561.

Kocin, P. J., P. N. Schumacher, R. F. Morales, and L. W. Uccellini, 1995: Overview of the 12–14 March 1993 superstorm. *Bull. Amer. Meteor. Soc.,* **76,** 165–182.

Lapenta, W. M., and N. L. Seaman, 1992: A numerical investigation of east coast cyclogenesis during the cold-air damming event of 27–28 February 1982. Part II: Importance of physical mechanisms. *Mon. Wea. Rev.,* **120,** 52–76.

Lefevre, R. J., and J. W. Nielsen-Gammon, 1995: An objective climatology of mobile troughs in the Northern Hemisphere. *Tellus,* **47A,** 638–665.

Petterssen, S., 1956: *Weather Analysis and Forecasting.* 2d ed. Vol. 1, *Motion and Motion Systems,* McGraw-Hill, 428 pp.

Rotunno, R., and M. Fantini, 1989: Petterssen's ''type B'' cyclogenesis in terms of discrete, neutral Eady modes. *J. Atmos. Sci.,* **46,** 3599–3604.

——, and J.-W. Bao, 1996: A case study of cyclogenesis using a model hierarchy. *Mon. Wea. Rev.,* **124,** 1051–1066.

Sanders, F., 1986: Explosive cyclogenesis in the west-central North Atlantic Ocean, 1981–84. Part I: Composite structure and mean behavior. *Mon. Wea. Rev.,* **114,** 1781–1794.

——, 1988: Life histories of mobile troughs in the upper westerlies. *Mon. Wea. Rev.,* **116,** 2629–2648.

——, and J. R. Gyakum, 1980: Synoptic-dynamic climatology of the ''bomb.'' *Mon. Wea. Rev.,* **108,** 1589–1606.

Uccellini, L. W., 1990: Processes contributing to the rapid development of extratropical cyclones. *Extratropical Cyclones: The Erik Palmen Memorial Volume,* C. W. Newton and E. O. Holopainen, Eds., Amer. Meteor. Soc., 81–105.

——, P. J. Kocin, R. S. Schneider, P. M. Stokles, and R. A. Dorr, 1995: Forecasting the superstorm of 12–14 March 1993. *Bull. Amer. Meteor. Soc.,* **76,** 183–199.

Whitaker, J. S., and A. Barcilon, 1992: Type B cyclogenesis in a zonally varying flow. *J. Atmos. Sci.,* **49,** 1877–1892.

Zou, X., Y.-H. Kuo, and S. Low-Nam, 1998: Medium-range prediction of an extratropical oceanic cyclone: Impact of initial state. *Mon. Wea. Rev.,* **126,** 2737–2763.